Available online at www.sciencedirect.com
ScienceDirect
Journal of Economic Theory 143 (2008) 541–557
JOURNAL OF Economic Theory
www.elsevier.com/locate/jet

Growing through chaotic intervals

Laura Gardini [a,*], Iryna Sushko [b], Ahmad K. Naimzada [c]

[a] *Department of Economics, Urbino University, Italy*
[b] *Institute of Mathematics, NASU, Kiev, Ukraine*
[c] *Università degli Studi di Milano-Bicocca, Italy*

Received 2 November 2007; final version received 8 March 2008; accepted 19 March 2008

Available online 28 May 2008

Abstract

We consider a growth model proposed by Matsuyama [K. Matsuyama, Growing through cycles, Econometrica 67 (2) (1999) 335–347] in which two sources of economic growth are present: the mechanism of capital accumulation (Solow regime) and the process of technical change and innovations (Romer regime). We will shown that no stable cycle can exist, except for a fixed point and a cycle of period two. The Necessary and Sufficient conditions for regular or chaotic regimes are formulated. The bifurcation structure of the two-dimensional parameter plane is completely explained. It is shown how the border-collision bifurcation leads from the stable fixed point to pure chaotic regime (which consists either in 4-cyclical chaotic intervals, 2-cyclical chaotic intervals or in one chaotic interval).

JEL classification: O41; E32; C62

Keywords: Cycles; Chaotic intervals; Border-collision bifurcation; Growth; Innovation

1. Introduction

In this work we consider the model first proposed by Matsuyama in [9], which describes the interaction of two sources of economic growth: The mechanism of capital accumulation and the process of technical change and innovation. Matsuyama constructed a one-dimensional dynamic model described by two different functions, each of which characterizes a different regime: The Solow regime, with high rates of growth, no innovations and a competitive market structure, as

* Corresponding author. Fax: +39 0722 305550.
E-mail address: laura.gardini@uniurb.it (L. Gardini).

0022-0531/$ – see front matter
doi:10.1016/j.jet.2008.03.005

in the neoclassical model, and the Romer regime, with low rates of growth, innovations and a monopolistic market structure, as in the neo-shumpeterian model. In this model the dynamics often alternates between the two different regimes: There is a trade off between growth and innovation. Analytically the model is represented by a piecewise smooth unimodal map, $x_{t+1} = \phi(x_t)$, where the function $\phi(x)$ is given by

$$\phi(x) = \begin{cases} f(x) = Gx^{1-\frac{1}{\sigma}} & \text{if } 0 < x < 1 \text{ (Solow regime)}, \\ g(x) = \frac{Gx}{1+\theta(x-1)} & \text{if } x > 1 \text{ (Romer regime)} \end{cases} \tag{1}$$

with $\theta = (1 - \frac{1}{\sigma})^{1-\sigma}$, and $\sigma > 1$. The independent variable x_t corresponds to the independent variable k_t in the original paper [9], that is, $x_t = \frac{K_t}{N_t \sigma F \theta}$ where K_t stands for capital, N_t the number of types of intermediate goods introduced up to time t, and F is some constant. The output Y_t is related to the amount of capital K_t, and the available types of intermediates, N_s, $0 < s < t$, through a production function. The model is closed assuming that a constant proportion of the output, Y_t, is left to be used as capital in the next period. When the state is $x_t < 1$ then no innovation occurs and no new intermediates are introduced, the vice versa takes place in the case $x_t > 1$. The two parameters of the model are G and σ. Increasing G the gross rate of growth changes, the fixed point from the Solow region ($0 < x < 1$) enters the Romer region ($x > 1$) and for $\sigma > 2$ is destabilized. The parameter σ denotes the demand elasticity of the intermediate good (and the monopoly margin), and also has a meaning in determining the share of labor ($\frac{1}{\sigma}$).

Matsuyama in [9] proved that the model may have stable or unstable equilibria, and that the dynamics may oscillate alternatively between the Solow regime and the Romer regime, when there is a stable 2-cycle. It was also shown that the 2-cycle may loose its stability, leading to different dynamic behaviors, when the parameter G belongs to the range $(1, (\theta - 1))$. The feasibility of growing through 2-cycles at rates faster than at the steady state was also established therein. The author also suggested that complex dynamic behaviors may occur, although a 3-cycle cannot exist.

This kind of dynamics stimulated further researchers: Mitra in [10] proves that topological chaos may occur in (1), at least when the parameter σ is quite high (he gives an example with $\sigma = 50$). The sufficient condition in the theorem proved in [10] is that the third iterate of the maximum is a point below the fixed point of the Romer regime. This condition, in other words, is exactly the condition for which the fixed point has homoclinic trajectories.[1] The example proposed by Mitra occurs at a high value of σ, while following Matsuyama the range of plausible values of σ is $(5, 20)$ (and as the most feasible value he suggested $\sigma = 6$). Then Mukherji in [11] showed that the condition for topological chaos may be satisfied also at lower values of σ (with respect to the one, 50, used by Mitra), giving an example at $\sigma = 22$. He also investigated the stability of the existing 2-cycle (giving the range of parameter values at which it is stable), suggesting that the transition to chaos may occur via the standard period-doubling bifurcation sequence, writing about a stable 4-cycle found after the destabilization of the 2-cycle, which we show not possible.

As we shall see in the present paper, the only stable cycles of the model in (1) are fixed points and 2-cycles. Any other existing cycle is unstable. So, what is the transition to chaos occurring in the model in (1)? It cannot be the standard flip-bifurcation sequence because stable cycles of even period, different from a 2-cycle, cannot occur. The object of the present work is to clarify completely the bifurcation conditions and the bifurcation mechanism occurring in this model,

[1] This condition implies topological chaos, that was proved by Devaney in [2], see also a different proof by Gardini in [4].

showing that indeed, for $G \in (1, (\theta - 1))$ the alternatives between the Solow and Romer regimes can occur in only two ways: Either the 2-cycle is stable, in which case any initial condition (i.c. for short henceforth) different from the fixed points converges towards the 2-cycle (and thus the Solow and Romer regimes alternate each time), or the dynamics are chaotic in the sense of "pure chaos," not only of topological chaos (which may also coexist with attracting cycles). However, the economic interpretation is not lost in such chaotic regions. On the contrary, it is enforced, as we shall clarify in the following.

In [9] and in [11] the authors emphasized that for $G < 1$ the Solow regime is globally stable (except for the origin), and noticed that for $G > (1 - \theta)$ the fixed point in the Romer regime is asymptotically stable and globally attracting (except for the origin). The interesting regime, not completely understood up to now, is the interval $1 < G < (\theta - 1)$, and nobody has commented about the bifurcation occurring at $G = 1$, except to say that for $G = 1$ the fixed point in the Solow regime ceases to exist. But what occurs as the value of G exceeds 1? We shall see that indeed this is not a standard bifurcation. It is a so-called *border-collision bifurcation*,[2] namely, the fixed point in the Solow regime is not going to become unstable because of its eigenvalue (and in fact also at the bifurcation value $G = 1$ the fixed point attracts all the points with i.c. $x > 0$). It collides with the border of its region of definition (the fixed point reaches the critical value $x = 1$), after which it does not exist any longer, but this collision gives rise to new dynamic behavior for a generic trajectory. The kinds of trajectories that we can have after the globally stable Solow regime depend on the value of the parameter σ. We shall see that at fixed $G = 1$ the region $\sigma > 1$ is divided in five intervals such that the border-collision bifurcation results in five different dynamic regimes (increasing the value of G) which are the following:

(1) *an attracting fixed point in the Romer regime if* $1 < \sigma < 2$;
(2) *an attracting* 2*-cycle if* $2 < \sigma < \sigma_4 \simeq 3.825$;
(3) *attracting* 4*-cyclical chaotic intervals if* $\sigma_4 < \sigma < \sigma_2 \simeq 6.123$;
(4) *attracting* 2*-cyclical chaotic intervals if* $\sigma_2 < \sigma < \sigma_1 \simeq 21.231$;
(5) *an attracting chaotic interval if* $\sigma > \sigma_1$.

As we can see, the value $\sigma = 6$ suggested by Matsuyama belongs to the third interval as well as the value $\sigma = 5$ used as a guiding example by Mukherji, which we also shall use in our examples. Indeed it makes no difference. Both values of σ (5 and 6) belong to the same interval, so the dynamic behavior of the model, as a function of G, is qualitatively the same. The range $(5, 20)$ of plausible values of σ involves only the intervals (3) and (4) given above, and as an example in the interval (4) we shall use $\sigma = 15$.

This work is organized as follows. In Section 2 we shall describe the dynamics of the model and the route to chaos, following the analysis of the previous authors (in [9] and in [11]), showing what occurs when the parameter σ is fixed and G is decreased from $G = (\theta - 1)$. Although the bifurcations related to the fixed point and the 2-cycle have already been investigated by other authors, here we give a different proof showing that these bifurcations are *critical flip bifurcations* and also *border-collision bifurcations*, writing a new analytical expression of the bifurcation curves. This technique allow us to obtain the formal expressions of all the bifurcations curves in the two-dimensional parameter plane (G, σ). Besides the two mentioned above (critical

[2] This kind of bifurcation is a quite recent topic of research. We refer to Hommes and Nusse [6], Maistrenko et al. [7,8], Nusse and Yorke [12,13], di Bernardo et al. [3], Banerjee et al. [1], Halse et al. [5], Sushko et al. [14,15], for some works related to one-dimensional piecewise smooth maps.

flip bifurcations which are also border-collision), the other two bifurcation curves are related to homoclinic bifurcations (of the 2-cycle and of the fixed point), and their implicit equation is given. The proof of the theorem on the border-collision bifurcation occurring in the model at the bifurcation value $G = 1$ is given in Section 3, and is performed by using a standard "normal form" already studied for piecewise linear one-dimensional maps. Section 4 concludes, showing how the economic interpretation of the model persists. In fact, for values of the parameters in the intervals (3) and (4), even if there are no stable cycles the dynamic behavior may be considered predictable from a macroscopic point of view and locally subject to small random shocks. This is because the trajectories visit 2-cyclic or 4-cyclic intervals, known in size and in sequence, and inside them the orbit behaves as in presence of small random shocks (although the model is completely deterministic, and no random shocks are exogenously given).

2. Properties of the model

2.1. Attracting fixed points

Let us consider the piecewise smooth map $x_{t+1} = \phi(x_t)$ given in (1). It is easy to see that for $1 < \sigma < \infty$ we have $1 < \theta < e$, and this is the range of interest: $\sigma > 1$. The function $f(x)$ on the left side (Solow regime) is monotonic increasing, because $f'(x) = G(1 - \frac{1}{\sigma})x^{-\frac{1}{\sigma}} > 0$. It has a unique fixed point $x_L^* = G^\sigma$ which exists (in its region of definition: $x < 1$) as long as $G < 1$, and when it exists, it is always stable, as $0 < f'(x_L^*) = (1 - \frac{1}{\sigma}) < 1$. Furthermore, it is globally attracting except for the origin. As the origin is always a repelling fixed point, we have restricted our interval of interest to $x > 0$. As mentioned in the Introduction, at $G = 1$ a bifurcation occurs, and for $G > (\theta - 1)$ the fixed point in the Romer regime ($x > 1$) is globally asymptotically stable. In fact, the function $g(x)$ defining the regime for $x > 1$ is monotonic decreasing and convex (as $g'(x) = -\frac{G(\theta-1)}{(1+\theta(x-1))^2} < 0$, and $g''(x) > 0$) and it has a unique fixed point $x_R^* = 1 + \frac{G-1}{\theta}$ which exists (in its region: $x > 1$) for any $G > 1$, but it may be stable or unstable. From $g'(x_R^*) = -(\frac{\theta-1}{G})$ we have that it is locally stable for $G > (\theta - 1)$, and it is easy to see that it is also globally attracting.

In Fig. 1a, we show the shape of the function $\phi(x)$ when the fixed point x_L^* is globally attracting ($G < 1$), while in Fig. 1b, x_R^* is globally attracting ($G > (\theta - 1)$). We also see immediately that at the bifurcation value $G = 1$, when the fixed point is $x^* = 1$, we have the left side derivative of the function $\phi'_L(1) = (1 - \frac{1}{\sigma}) < 1$ and independently on the value of the derivative of the function on the right, this is enough to prove that the fixed point $x^* = 1$ is globally attracting. In fact, any point with $x > 1$ is mapped in one iteration on the left side with $x < 1$ from which the iterations converge (increasing monotonically) to the fixed point $x^* = 1$. Similarly, due to the monotonicity of the functions on the right side for $G > (\theta - 1)$, with $g(1) = G$ and $g(G) = \frac{G^2}{1+\theta(G-1)} > 1$, we have that any point $x \in (0, 1)$ will reach the region $x > 1$ in a finite number of iterations, and the region $x > 1$ is mapped into itself, with the fixed point globally attracting.

2.2. Cycle of period 2

From the previous observations it follows that the interesting region is the interval $1 < G < (\theta - 1)$, and the dynamics of the model as G varies in this interval depend on the value of the other parameter σ. At the bifurcation value $G = (\theta - 1)$ all the points in the interval $[1, G]$ belong

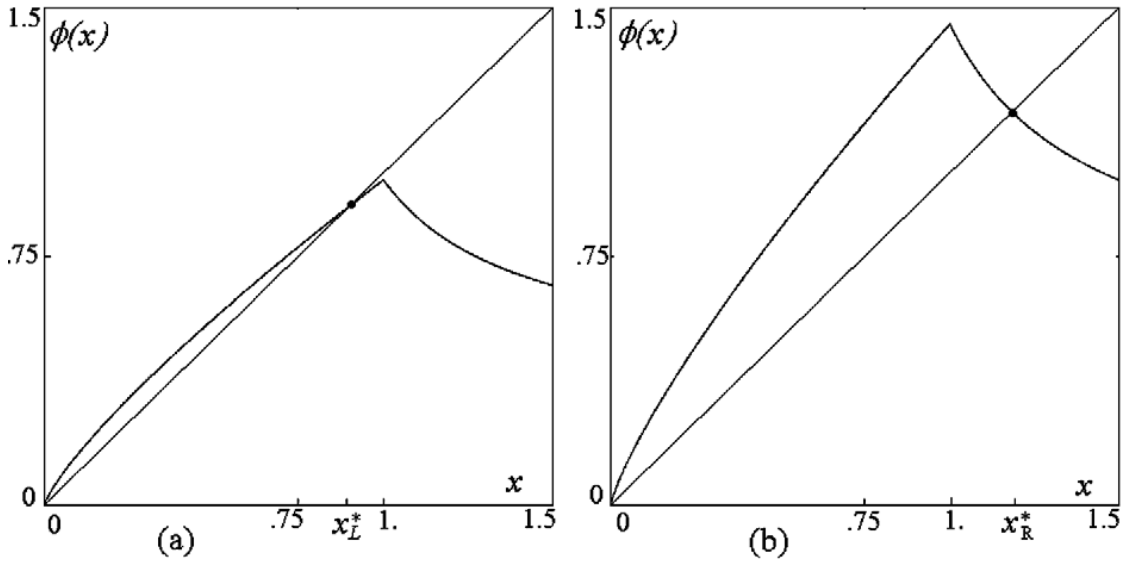

Fig. 1. The function $\phi(x)$ with the globally attracting fixed point x_L^* in the Solow regime at $G = 0.98$, $\sigma = 5$ (a), and x_R^* in the Romer regime at $G = 1.45$, $\sigma = 5$ (b).

to 2-cycles (stable but not asymptotically stable). In fact, the bifurcation value $G = (\theta - 1)$ is a critical flip bifurcation: all the points of the segments $[1, x_R^*)$ and $(x_R^*, 1]$ are 2-cycles. We can show this by using the change of variable which puts x_R^* in the origin. That is, let $y = x - x_R^*$ then

$$H_R(y) = g\left(y + x_R^*\right) - x_R^* = \frac{(1-\theta)y}{\theta y + G} \tag{2}$$

and

$$H_R^2(y) = H_R \circ H_R(y) = \frac{(1-\theta)^2 y}{y(\theta(1-\theta) + G\theta) + G^2} \tag{3}$$

so that at the bifurcation value $G = (\theta - 1)$ we have $H_R^2(y) = y$. Any i.c. with $x > 0$ will be mapped into the interval $[1, G]$ in a finite number of iterations, thus ending in a 2-cycle with both states in the Romer regime. It was also shown in [9] that for $G < (\theta - 1)$ there exists a 2-cycle, the dynamics "oscillate" between the Solow regime and the Romer regime, and the dynamics of the map in (1) always belong to the *absorbing interval* $[g(G), G]$. Any point with i.c. $x > 0$ will enter this interval in a finite number of iterations, from which it will never escape since $\phi([g(G), G]) \subseteq [g(G), G]$.

The rigorous proof of the bifurcations occurring in the map in (1) are not easy, because of the complex analytical expressions. However, a numerical proof can first be given. In Fig. 2 we present a two-dimensional bifurcation diagram in the (G, σ)-parameter plane in which different gray tonalities correspond to different dynamic regimes of the map (1).

Let us here consider the parameter values corresponding to the existence of a two-cycle. Since in the Romer regime the function $g(x)$ is decreasing and convex, we have that the first derivative $g'(x)$ is negative and it increases as x increases from 1 (but remaining $g'(x) < 0$). It follows that if the derivative in the critical point satisfies $-1 < g'(1)$ we must have $-1 < g'(x) < 0$ for any $x > 1$. From the expression $g'(1) = -G(\theta - 1)$ we have that $|g'(1)| < 1$ whenever both the conditions hold, $G < 1$ and $\theta \leqslant 2$, which corresponds to $\sigma \leqslant 2$. Moreover, in the (G, σ)-parameter plane the bifurcation curve of equation $G = (\theta - 1)$ issues from the point $(G, \sigma) = (1, 2)$ and is increasing and convex—as can be seen in Fig. 2 (this fact was also proven in [11]).

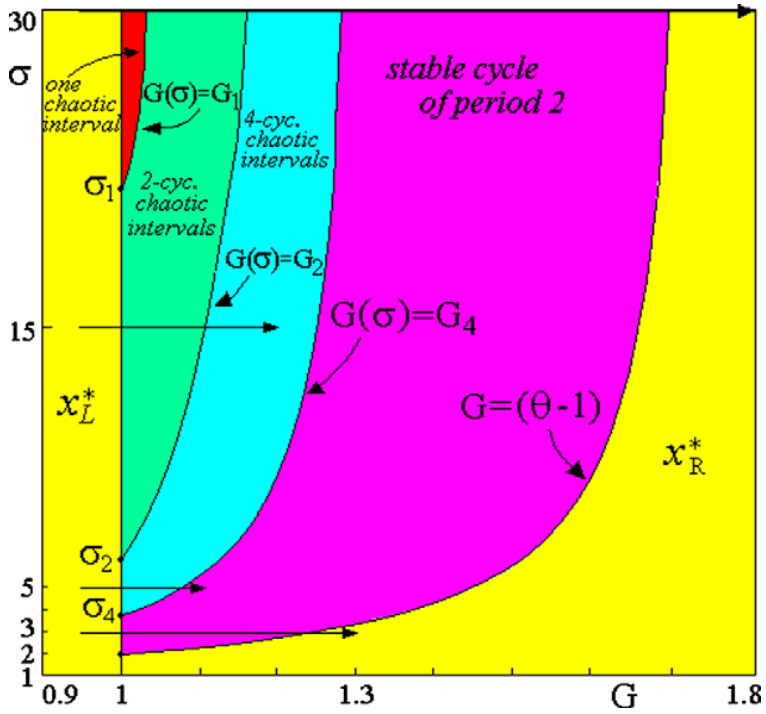

Fig. 2. Orbit (or bifurcation) diagram in the (G, σ)-parameter plane. The lightest gray color corresponds to the parameter values at which the map ϕ has a stable fixed point (which is x_L^* for $G < 1$, or x_R^* for $G > 1$, $G > (\theta - 1)$), followed by a strip related to the parameter values at which the map ϕ has an attracting cycle of period 2, and in sequence gray tonalities correspond to 4-, 2- and one-piece chaotic intervals, respectively. The horizontal lines with arrows denote paths followed in Figs. 6 and 7.

Thus, the line $\sigma = 2$ never intersects the bifurcation curve $G = (\theta - 1)$ (apart from the issuing point). So, all the interesting dynamics occur at fixed values of σ with $\sigma > 2$, otherwise we must have a stable fixed point (either on the left, if $G < 1$, or on the right, if $G > 1$). It follows that in order to detect a stable 2-cycle we must have $\sigma > 2$, which corresponds to $(\theta - 1) > 1$. Now let us assume that $\sigma > 2$ is fixed and G decreases, starting from some value $G > (\theta - 1)$ for which x_R^* is stable (see Fig. 2). Then, as we have seen above, the loose of stability of x_R^* occurs via a critical bifurcation: At the bifurcation value $G = (\theta - 1)$ all the points of a segment are 2-cycles. In particular $\{1, G\}$ forms a 2-cycle. After the bifurcation, for $G < (\theta - 1)$, the fixed point x_R^* is unstable. Furthermore no stable 2-cycle can exist with both the points on the right, in the Romer regime. This is proved by the fact that we have $g'(x) < -1$ for all the points x in the interval $[1, G]$, because in the iterated map $H_R \circ H_R(y)$ we have the slope equal to 1 in all the points of a segment (see Fig. 3a where $\phi(x)$ and $\phi^2(x)$ are shown at the bifurcation value $G = (\theta - 1)$), while after the bifurcation (see Fig. 3b, where $G < (\theta - 1)$) we have the slope greater than 1 in the segment $x \in [1, G]$.

This is rigorously proved by using

$$\frac{d}{dy} H_R^2(y) = \frac{(1-\theta)^2 G^2}{[y(\theta(1-\theta) + G\theta) + G^2]^2} = \frac{(\frac{1-\theta}{G})^2}{[\frac{y(\theta(1-\theta)+G\theta)}{G^2} + 1]^2}$$

from which we have $\frac{d}{dy} H_R^2(0) > 1$. Moreover, from $(\theta - 1) > G$, we have $\theta(\theta - 1) > G\theta$ so that $G\theta + \theta(1 - \theta) < 0$, and for y in a right neighborhood of 0 the denominator of $\frac{d}{dy} H_R^2(y)$ is less than 1, and thus $\frac{d}{dy} H_R^2(y) > (\frac{1-\theta}{G})^2 > 1$. From the considerations given above, it follows that a unique 2-cycle exists after the bifurcation, for $G < (\theta - 1)$, with one point of the cycle in the

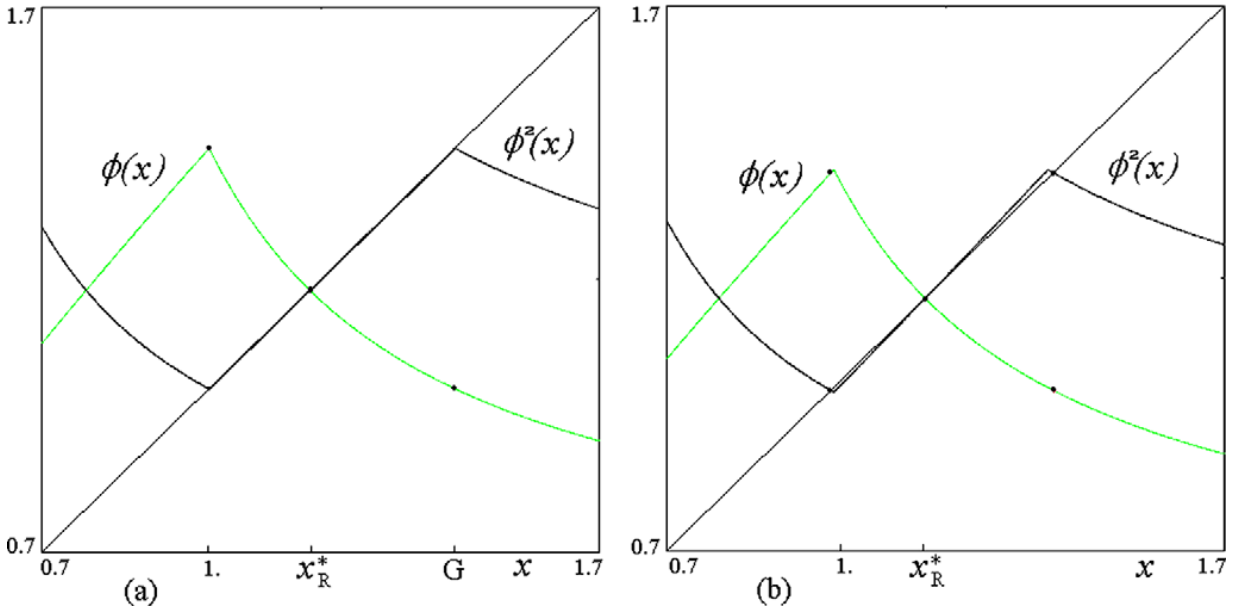

Fig. 3. The functions $\phi(x)$ and $\phi^2(x)$ at the critical flip bifurcation value $G = (\theta - 1) = 1.441408$, $\sigma = 5$ (a) and after, at $G = 1.4 < (\theta - 1)$ (b).

Solow regime and one point in the Romer regime, $\{x_L, x_R\}$. From stable (inside the wide region) it becomes unstable as G decreases reaching the value $G = G_4$ in Fig. 2. The local stability of this unique 2-cycle was already studied in [11], and a sufficient condition for its stability is given, depending on the points of the 2-cycle:

$$\left|\phi'(x_L)\phi'(x_R)\right| = \frac{x_L^{\frac{1}{\sigma}}(1-\frac{1}{\sigma})(\theta-1)}{G^2} < 1. \tag{4}$$

The bifurcation occurs when $|\phi'(x_L)\phi'(x_R)| = 1$ in (4), once that the explicit expression of x_L is there inserted, but this is not known, thus it is difficult to obtain an explicit form. However, a different way to get the bifurcation condition comes from considering the images of the critical point $x = 1$ (or equivalently of its first iterate $x = G$). It can be noticed that the bifurcation occurring at $G = (\theta - 1)$ increasing G, for the existing stable 2-cycle (with points $x_L < 1 < x_R$) corresponds to a border-collision bifurcation: The periodic point x_L merges with the critical point $x = 1$, which is a 2-cycle at this parameter value. The condition $G = (\theta - 1)$ may thus be written also as $\phi(G) = 1$ or $\phi^2(1) = 1$, which reads explicitly also as $g^2(1) = 1$. Similarly, at the bifurcation in which the stable 2-cycle becomes unstable as G decreases, one might think that a stable 4-cycle would appear. Let us first describe what occurs via an example. In Fig. 4a ($G = 1.1$), we show the same example considered by Mukherji ($\sigma = 5$) at a value of G in which the 2-cycle is stable. We can see that this corresponds to two stable fixed points for the iterated map $\phi^2(x)$. It can be also seen that the bifurcation structure is quite similar to the critical situation occurring at the bifurcation of the fixed point. That is, as G decreases approaching the bifurcation value, in the graph of $\phi^4(x)$ two segments tend to collide with the diagonal. In fact this can clearly be seen in Fig. 4b ($G = 1.073$), although the parameters are only close to the bifurcation value and the iterations of the critical point still tend to the stable 2-cycle. The bifurcation occurs at approximately $G = 1.0725$, as shown in Fig. 5a, where we have indeed that the points 1, G, $g(G)$, and $f \circ g(G)$ form a 4-cycle, and the points of the segments $[g(G), 1]$, $[f^{\circ}g(G), G]$ are all fixed points for the map $\phi^4(x)$ (corresponding to all 4-cycles for ϕ and only one 2-cycle with periodic points approximately in the center of the two intervals). It can be noticed that at the

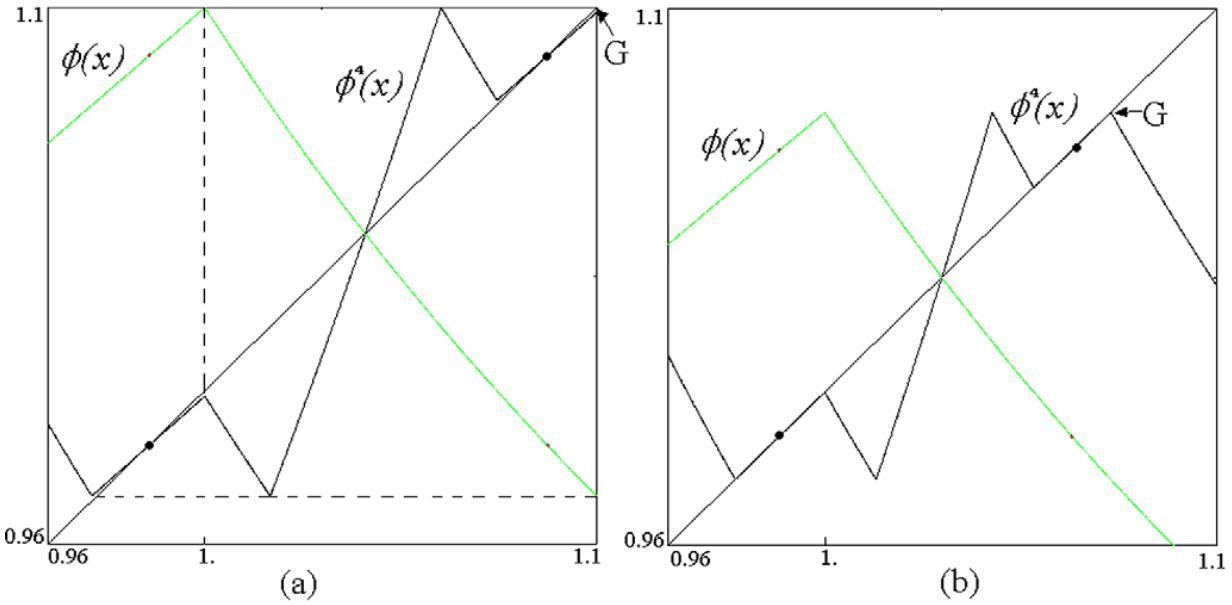

Fig. 4. The functions $\phi(x)$ and $\phi^4(x)$ at the parameter values $G = 1.1$, $\sigma = 5$ in (a) and $G = 1.073$, $\sigma = 5$ in (b), for which the map ϕ has the attracting 2-cycle.

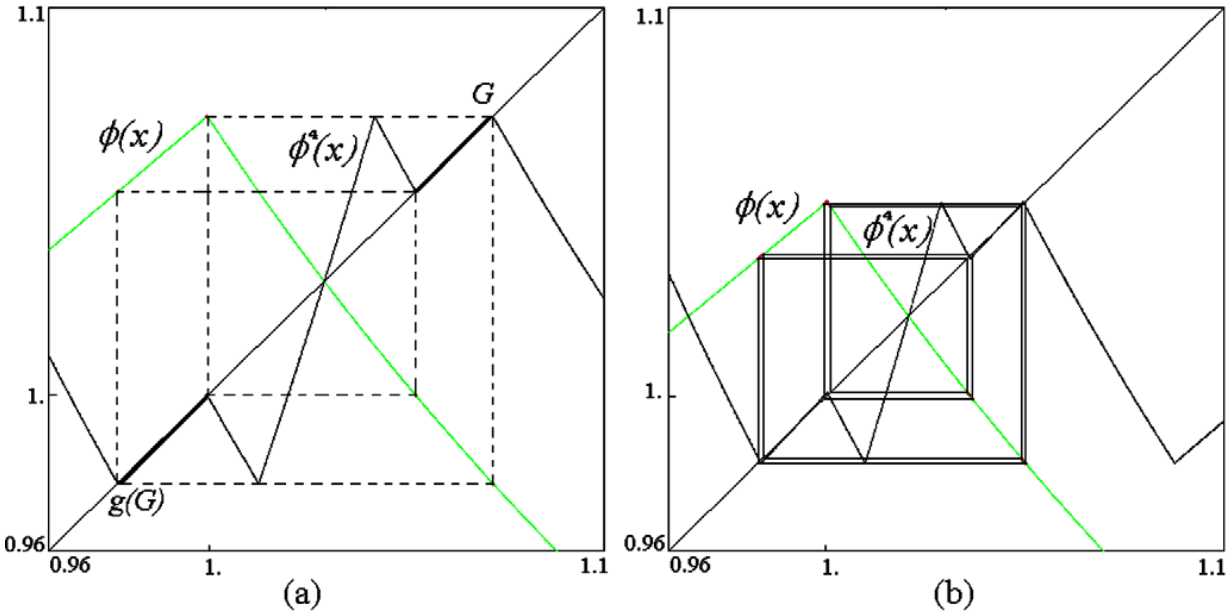

Fig. 5. The functions $\phi(x)$ and $\phi^4(x)$ at the parameter values $G = 1.0725$, $\sigma = 5$, are related approximately to the critical flip bifurcation of the 2-cycle in (a) and after the bifurcation, at $G = 1.05$, $\sigma = 5$, when the map ϕ has 4-cyclical chaotic intervals in (b).

bifurcation value, $|\frac{d}{dx}\phi^4(x)| \geqslant 1$ for all the points of the absorbing segment of the map, thus it is impossible to get a stable 4-cycle after the bifurcation. In fact, after the bifurcation (see Fig. 5b), also the segments previously on the diagonal now have slopes higher than 1, thus we have $|\frac{d}{dx}\phi^4(x)| > 1$ in all the points of the absorbing interval.

It turns out that a stable 4-cycle is impossible. Moreover, any cycle of any period cannot be stable, because ϕ^4 is expanding in the absorbing interval $[g(G), G]$. Instead, all the asymptotic trajectory inside this interval tend to the unique attractor, which is chaotic and made up of 4 cyclical chaotic intervals for the map ϕ (corresponding to four invariant chaotic intervals for ϕ^4),

which are bounded by the images of the critical point, that is: $\phi^i(1)$ for $i = 1, 2, \ldots, 8$ (i.e., $G, g(G), \ldots$). The considerations given above also show that the bifurcation condition in (4) is equivalent to the condition $\phi^4(1) = 1$ (the critical point must be periodic of period four), which is given by

$$g \circ f \circ g^2(1) = 1. \tag{5}$$

We can so state the following:

Proposition 1. *The stability region of the* 2*-cycle of the map in* (1)*, shown in Fig.* 2*, for any fixed value* $\sigma > 2$*, is bounded by the curves of implicit equations* $g^2(1) = 1$ (*which corresponds explicitly to* $G = (\theta - 1)$) *and* $g \circ f \circ g^2(1) = 1$ (*implicit equation for* $G(\sigma) = G_4$).

The critical bifurcation of the 2-cycle (related with its stability/instability) also corresponds to the bifurcation curve at which the 4 pieces chaotic intervals undergo a border collision bifurcation, and thus the condition is obtained either from $\phi^4(1) = 1$ which corresponds to the condition given in (5), or from the equality in (4) (but there, the coordinate of the point x_L of the 2-cycle is not analytically known). We have seen numerically that for any fixed value of $\sigma > \sigma_4$ ($\simeq 3.825$) the equation given in (5) has a single solution, which we have called G_4 in Proposition 1.

2.3. Chaotic intervals

Really the proof given in the previous subsection of the dynamics of the map is numerical, but the slopes of the function ϕ^4 in the absorbing interval are easy to see (as the pieces of the function look almost piecewise linear, and it is enough to compare the slopes with the two diagonals). So we state that also the bifurcation occurring for the attracting 2-cycle is critical (as it is proved for the fixed point), and no stable cycle can exist. Moreover, as it is easy to see numerically, the slopes become steepest as G further decreases towards 1, so the condition $|\frac{d}{dx}\phi^4(x)| > 1$ persists at any lower value of G up to 1. Thus no period-doubling bifurcation occurs at the 2-cycle as G decreases, crossing through the value $G = G_4$, at which the equation $g \circ f \circ g^2(1) = 1$, or equivalently $g \circ f \circ g(G) = 1$, holds, while chaotic regimes exist. Indeed, as we see in Fig. 2, it is also correct to say that cycles of period three cannot exist, but the chaotic regimes exist anyhow. As we have already mentioned in the introduction, the sufficient condition stated by Mitra in [10] can be enforced in terms of homoclinic trajectories. Let us recall the following statement (for the proof we refer to [2], Theorem 16.3, see also [4], Theorem 1):

Proposition 2. *Let* m *be the unique critical point of a continuous, piecewise smooth, unimodal map of an interval into itself, say* $F : I \to I$*,* $F(m)$ *maximum* (*resp. minimum*)*, with a unique unstable fixed point* x^**, and a sequence of preimages of* m *tends to* x^**. Then the first homoclinic orbits* (*all critical*) *of the fixed point* x^* *occur when the critical point satisfies* $F^3(m) = x^*$*. When the critical point is a local maximum* (*resp. minimum*) *then for* $F^3(m) < x^*$ (*resp.* $F^3(m) > x^*$) *infinitely many* (*noncritical*) *homoclinic orbits of the fixed point exist, and thus there is a closed invariant set* $X \subseteq [F^2(m), F(m)]$ (*resp.* $X \subseteq [F(m), F^2(m)]$) *on which the map is topologically conjugate to the shift automorphism, and thus* F *is chaotic, in the sense of topological chaos* (*with positive topological entropy*).

In the specific case of the model in (1) this condition clearly occurs when σ is big enough (as shown in [10] and in [11]), but we can say more. In fact, when the condition $\phi^3(1) = x_R^*$ is satisfied we have that the map is chaotic in the whole interval $[g(G), G]$. It is worth noticing that the

condition given above says nothing about the density of the chaotic set X. Indeed, X may also be a set of points of zero measure in I, and in such a case the chaotic dynamics, although existing, is not detectable by numeric simulations of a generic trajectory. The situation is different when the chaotic set is an interval or cyclical chaotic intervals (as it occurs, for example, at the condition $F^3(m) = x^*$ stated above, when all the homoclinic orbits of x^* are critical). The appearance of such *full measure chaotic intervals* is indeed what occurs in our model (1) whenever the fixed point and the 2-cycle are not stable, as stated in the following

Proposition 3. *For any fixed value $\sigma > 2$ when the fixed point and the 2-cycle of the map in* (1) *are unstable, the attractors are full measure chaotic intervals.*

In fact, the dynamics which may occur as G is further decreased below the value $G = G_4$ are always chaotic: After the 2-cycle, 4-cyclical chaotic intervals appear, which may merge (say at $G = G_2$) into 2-cyclical chaotic intervals, which in turn may merge (say at $G = G_1$) into one chaotic interval (see Fig. 2).

The bifurcation curve at which 4-cyclical chaotic intervals merge in pairs into 2-pieces chaotic intervals (and vice versa) is *the first homoclinic bifurcation of the repelling 2-cycle* (which was external to the four chaotic intervals). Thus we also have the condition for detecting this homoclinic bifurcation (Proposition 2 applied to the iterated map ϕ^2). That is, this bifurcation occurs when $\phi^6(1) = (\phi^2)^3(1) = x_L$ in the Solow regime or, equivalently, when the fifth iterate of the point of maximum ($x = 1$) merges into the periodic point x_R in the Romer regime, $\phi^5(1) = x_R$, which corresponds to

$$g^2 \circ f \circ g^2(1) = x_R. \tag{6}$$

Although it is quite complicated to find it in explicit form analytically, we have numerically seen that for any fixed value of $\sigma > \sigma_2$ ($\simeq 6.123$) the equation given in (6) has a single solution, which we call G_2.

The 2-cyclical chaotic intervals are always bounded by the images of the critical point (now $\phi^i(1)$ for $i = 1, 2, 3, 4$, i.e., $G, g(G), \ldots$, that is $[g(G), g \circ f \circ g(G)]$, $[f \circ g(G), G]$). However this does not occur at the low value of σ (as $\sigma = 5$ in the above example). Indeed the chaotic regime may not be reached either, as can be seen also from Fig. 2. The dynamic behaviors of the map as G decreases or increases depend on the value of σ, for $2 < \sigma < \sigma_4$ we can only have a stable 2-cycle and chaotic intervals never occur at any value of G, while chaotic intervals occur for any $\sigma > \sigma_4$.

To illustrate the dynamic behavior let us show a few figures of one-dimensional bifurcation diagrams (or orbit diagrams) at fixed values of σ. Figs. 6, 7 show the asymptotic behavior of the state variable x (in the vertical axis) as a function of G (in the horizontal axis). As already remarked, it is worth noticing that whichever is the value of σ, as is easy to see from the analytical expression of $g(G)$, as G tends to 1 $g(G)$ also tends to 1, so that the whole absorbing interval $[g(G), G]$ shrinks to one point, the point of maximum $x = 1$ and also maximum value $G = 1$ (and attracting fixed point). Each figure represents the dynamics occurring at a cross-section of the bifurcation diagram in Fig. 2, at fixed values of σ (the cross-sections are indicated in Fig. 2 by the straight lines with arrows). The bifurcation curves represented there, separating the different kinds of chaotic intervals, have been done numerically, by using the analytical conditions related with the homoclinic bifurcations of the relevant cycles. One is the equation given in (6), while the bifurcation curve at which 2 pieces chaotic intervals merge into a single one (or vice versa a chaotic interval splits into two cyclical chaotic intervals) occurs *when the fixed point in the*

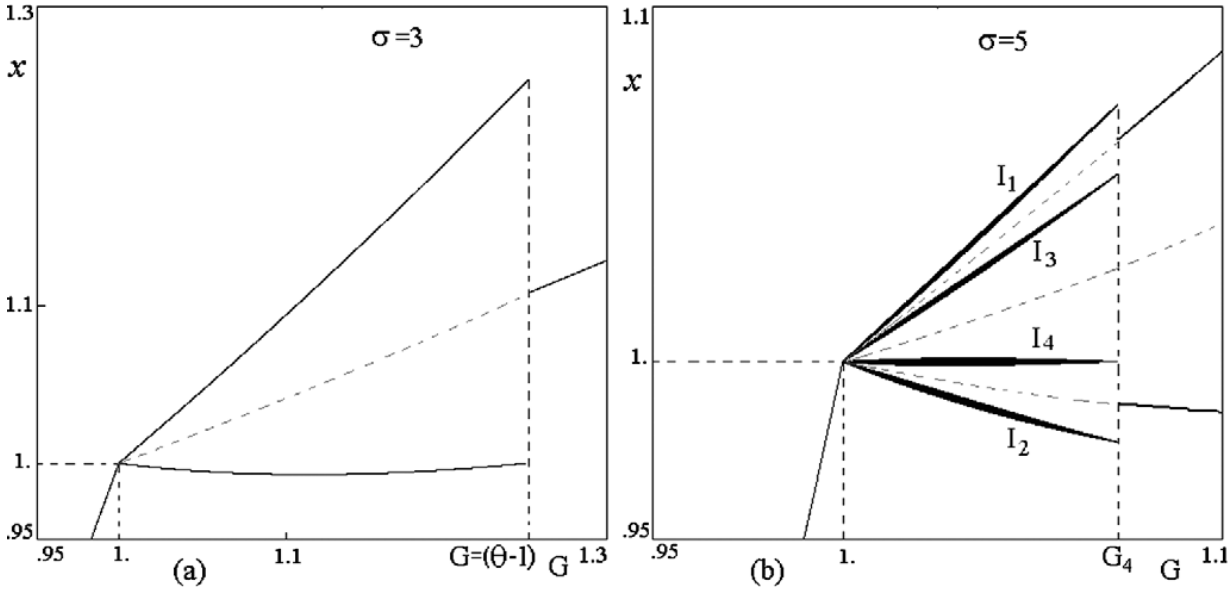

Fig. 6. One-dimensional bifurcation diagrams of the map ϕ. $\sigma = 3$, $g \in [0.95, 1.3]$, in (a); $\sigma = 5$, $g \in [0.95, 1.1]$, in (b).

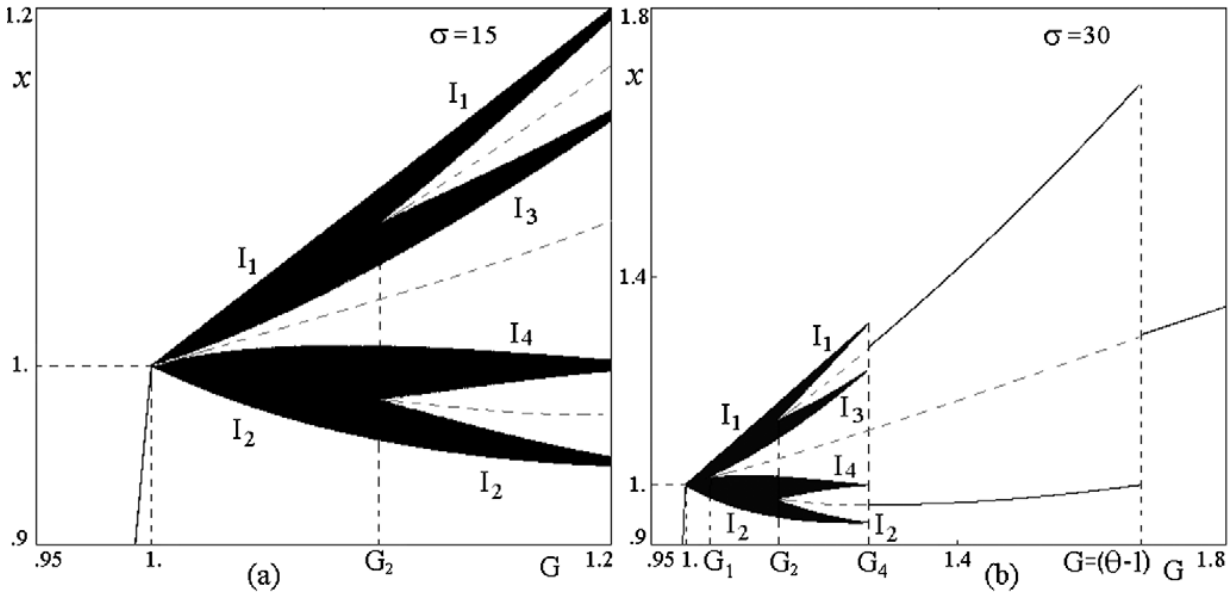

Fig. 7. One-dimensional bifurcation diagrams of the map ϕ. $\sigma = 15$, $g \in [0.95, 1.2]$, in (a); $\sigma = 30$, $g \in [0.95, 1.8]$, in (b).

Romer regime becomes homoclinic (by Proposition 2). So the condition is obtained when the third iterate of the point of maximum ($x = 1$) merges into the fixed point, $\phi^3(1) = x_R^*$, which in our case corresponds to

$$f \circ g^2(1) = x_R^*, \tag{7}$$

i.e. $f \circ g(G) = x_R^*$, and more explicitly reads as follows:

$$G\left(\frac{G^2}{1+\theta(G-1)}\right)^{(1-\frac{1}{\sigma})} = 1 + \frac{G-1}{\theta}. \tag{8}$$

We have seen numerically that for any fixed value of $\sigma > \sigma_1$ ($\simeq 21.231$) the equation given in (8) has a single solution, which we call G_1 (for example, at $\sigma = 50$, value used by Mitra, we have

$G_1 = 1.024254692$, at $\sigma = 22$, value used by Mukherji, we have $G_1 = 1.001468146$, at $\sigma = 30$, value used in the bifurcation diagram in Fig. 7b we have $G_1 = 1.0123131$).

3. Border-collision bifurcation at $G = 1$

We have seen before that the bifurcations occurring at the fixed point and the 2-cycle, which are critical bifurcations, may also be considered as border-collision bifurcations. In fact, the bifurcation of the fixed point occurring for any value of $\sigma > 2$ at $G = (\theta - 1)$, may be characterized as $\phi^2(1) = 1$, and the critical bifurcation of the 2-cycle (related with its stability/instability) also corresponds to the bifurcation curve at which 4 pieces chaotic intervals undergo a border collision bifurcation, and thus the condition is $\phi^4(1) = 1$. However, the main role of the border-collision bifurcation is clearly the one observed in the model when, at a fixed values of σ, the parameter G is increased and the stable fixed point in the Solow regime merges the point $x = 1$. The kinds of dynamics that will be observed after the border-collision bifurcation occurring at $G = 1$ comes from the following

Theorem. *The border-collision bifurcation of the fixed point $x^* = 1$ of the map ϕ given in* (1)*, occurring at $G = 1$ for any $\sigma > 1$, gives rise* (*as G increases*) *to*

- *an attracting fixed point x_R^* if $1 < \sigma < 2$;*
- *an attracting cycle of period* 2 *if $2 < \sigma < \sigma_4 \simeq 3.825$;*
- *attracting* 4*-cyclical chaotic intervals if $\sigma_4 < \sigma < \sigma_2 \simeq 6.123$;*
- *attracting* 2*-cyclical chaotic intervals if $\sigma_2 < \sigma < \sigma_1 \simeq 21.231$;*
- *an attracting chaotic interval if $\sigma > \sigma_1$.*

Proof. The theorem can be proved by using the normal form of the border-collision bifurcation occurring in one-dimensional piecewise smooth maps first proposed in [13]. According to Theorem 3 stated in [13] applied to the map ϕ given in (1), the result of the border-collision bifurcation of the fixed point depends on the left and right side derivatives of $\phi(x)$ evaluated at $x = 1$ for $G = 1$, here denoted α and β, respectively:

$$\alpha = \lim_{x \to 1_-} \frac{d}{dx}\phi(x), \qquad \beta = \lim_{x \to 1_+} \frac{d}{dx}\phi(x). \tag{9}$$

The related normal form is given by the skew-tent map $\psi : \mapsto \psi(y)$ defined by the function

$$\psi(y) = \begin{cases} \alpha y + \varepsilon, & y \leqslant 0, \\ \beta y + \varepsilon, & y \geqslant 0. \end{cases} \tag{10}$$

Here ε is a bifurcation parameter such that as ε varies through 0, the local bifurcations of the piecewise linear map ψ and the piecewise smooth map ϕ are of the same kind. That is, the border-collision bifurcation occurring for the fixed point $x^* = 1$ of the map ϕ at $G = 1$ is of the same kind as the border-collision bifurcation of the fixed point $y^* = 0$ of the map ψ occurring at $\varepsilon = 0$.

The dynamics of the piecewise linear map ψ have already been studied (see [1,7], and references therein), and depend on the slopes α and β of the linear functions. All the possible kinds of border-collision bifurcation of the fixed point x^* are classified according to the partition of the (α, β)-parameter plane into subregions in which the same qualitative dynamics take place. We summarize these results in Fig. 8, which schematically shows the related one-dimensional bifurcation diagrams for the border-collision of the fixed point of the map ψ. The cases $0 < \alpha < 1$,

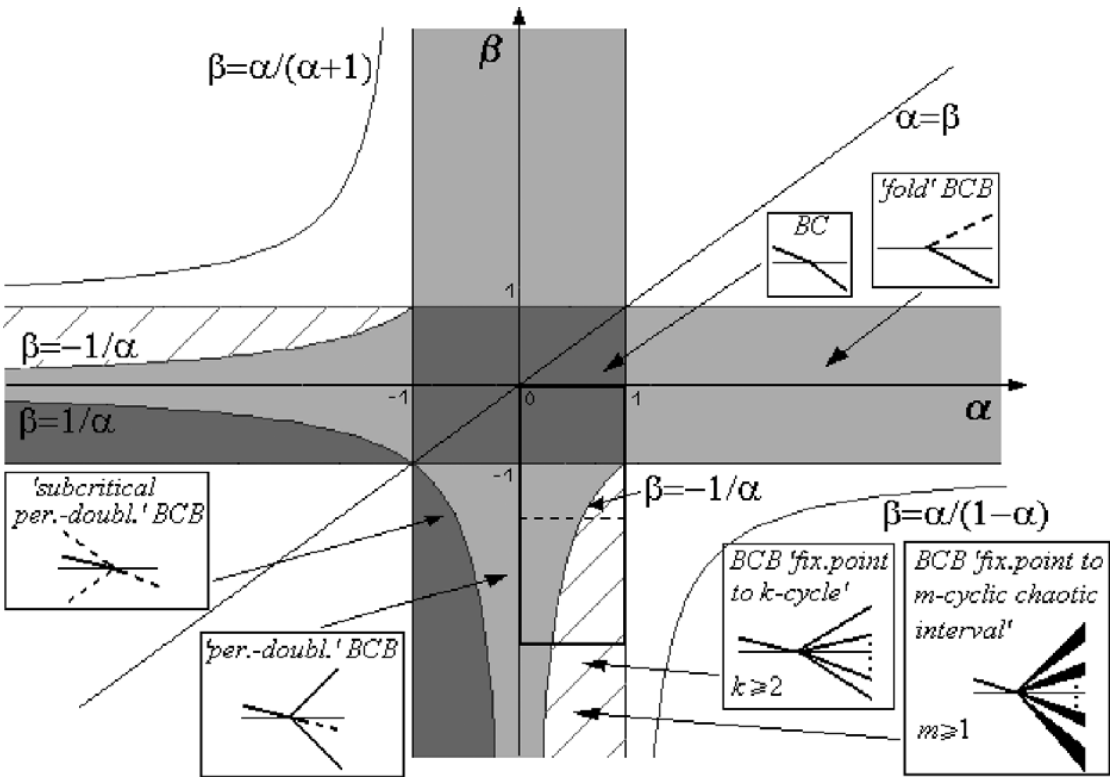

Fig. 8. The partition of the (α, β)-parameter plane into the regions with qualitatively similar dynamics of the map ψ at $\varepsilon < 0$ (for $\beta > \alpha$) and at $\varepsilon > 0$ (for $\beta < a$). Corresponding border-collision bifurcations of the fixed point of ψ, occurring at $\varepsilon = 0$ as ε varies from $\varepsilon < 0$ to $\varepsilon > 0$, are shown schematically by means of one-dimensional bifurcation diagrams (the same kinds of BCB occur for $\alpha < \beta$ as ε varies from $\varepsilon > 0$ to $\varepsilon < 0$): The thick and dashed lines indicate attracting and repelling cycles, respectively. The thin lines correspond to the border point.

$\beta < -1$, and $\alpha < -1$, $0 < \beta < 1$ (see the dashed regions in Fig. 8), have been studied by many authors. They are qualitatively the same case due to the symmetry of the (α, β)-parameter plane with respect to the line $\alpha = \beta$. It has been shown that for $\varepsilon > 0$ ($\varepsilon < 0$, respectively), all trajectories are bounded and the map ψ can have an attracting cycle of any period $k \geqslant 2$, denoted q_k, as well as a cyclic chaotic interval of any period $m \geqslant 1$, denoted Q_m. This means that varying ε through 0 from $\varepsilon < 0$ to $\varepsilon > 0$ (from $\varepsilon > 0$ to $\varepsilon < 0$, respectively) we can have the border-collision bifurcation from the attracting fixed point x^* to any one of such attractors. The region $\alpha > 1, \alpha/(1-\alpha) < \beta < -1$ (and $\alpha < -1, 1 < \beta < \alpha/(\alpha+1)$) includes subregions corresponding to the transition from no attractor to cyclic chaotic intervals Q_m of period $m = 2^k$, $k = 0, \ldots, l$, where $l \to \infty$ as $(\alpha, \beta) \to (1, -1)$ ($(\alpha, \beta) \to (-1, 1)$, respectively).

Now we write the coefficients of the normal form (10) in terms of the parameter σ. From (9) we get

$$\alpha = \left(1 - \frac{1}{\sigma}\right), \qquad \beta = (1 - \theta) \tag{11}$$

so that we have $0 < \alpha < 1$ and $\beta < 0$. Moreover, from $1 < \theta < e$ we have that $1 - e < \beta < 0$. Thus, the region of our interest in the (α, β)-parameter plane is $0 < \alpha < 1$, $1 - e < \beta < 0$ (see the thick rectangle in Fig. 8). Substituting first $\theta = (1 - \frac{1}{\sigma})^{1-\sigma}$ and then $\sigma = 1/(1-\alpha)$ into (11) we get the expression of the border-collision curve of the fixed point $x^* = 1$ in terms of the parameters α and β, which is denoted as $\mathcal{B}$,

$$\mathcal{B}: \quad \beta = 1 - \alpha^{\alpha/(\alpha-1)}. \tag{12}$$

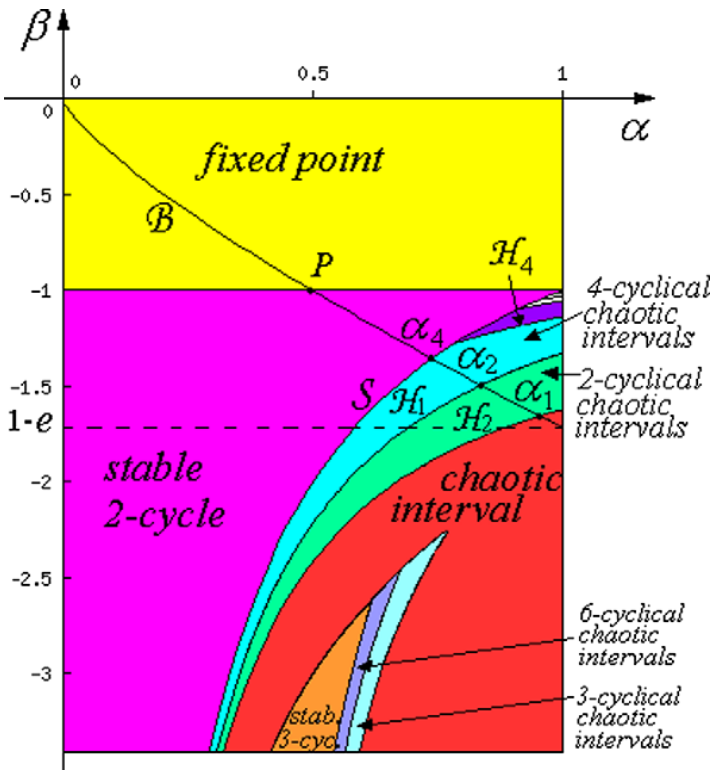

Fig. 9. The enlarged window of Fig. 8, where the border-collision bifurcation curve $\mathcal{B}$ of the fixed point $x^* = 1$ of the map ϕ is shown, as well as the critical flip bifurcation curve $\mathcal{S}$ of the 2-cycle of the map ψ, the homoclinic bifurcation curves $\mathcal{H}_i$, $i = 1, 2, 4$, of the corresponding cycles of ψ and the bifurcation curves related to the 3-cycle of ψ.

Fig. 9 presents an enlargement of the rectangle of interest in Fig. 8, and in it the curve $\mathcal{B}$ is shown. By using the analytic expressions of the bifurcation curves as given in [7], we can describe the regions of the (α, β)-parameter plane which are crossed by the curve $\mathcal{B}$. We can see that $\mathcal{B}$ intersects:

(1) the straight line $\beta = -1$ at a point P which is $(\alpha, \beta) = (0.5, -1)$, related to the (critical) flip bifurcation of the fixed point y^*;

(2) the curve, denoted as $\mathcal{S}$, given by

$$\mathcal{S}: \quad \beta = -\frac{1}{\alpha},$$

related to the (critical) flip bifurcation of the 2-cycle (after which the curve $\mathcal{B}$ enter a region of 4-cyclical chaotic intervals). The intersection point is denoted by α_4, i.e., $\mathcal{B} \cap \mathcal{S} = \alpha_4$;

(3) the curve, denoted as $\mathcal{H}_2$, given by

$$\mathcal{H}_2: \quad \alpha = \frac{-1 - \sqrt{1 + 4\beta^4}}{2\beta^3},$$

which is related to the homoclinic bifurcation of the 2-cycle of the map ψ giving rise to the transition from 4-cyclical chaotic intervals to 2-cyclical chaotic intervals, $\mathcal{B} \cap \mathcal{H}_2 = \alpha_2$;

(4) the curve denoted as $\mathcal{H}_1$ given by

$$\mathcal{H}_1: \quad \beta = \frac{-1 + \sqrt{1 + 4\alpha^2}}{2\alpha},$$

which is related to the homoclinic bifurcation of the fixed point y^* of the map ψ, giving rise to the transition from 2-cyclical chaotic intervals to one chaotic interval; $\mathcal{B} \cap \mathcal{H}_1 = \alpha_1$.

Other bifurcation curves are also shown in Fig. 9, not intersected by $\mathcal{B}$. For example the curve $\mathcal{H}_4$ corresponding to the transition from 4-cyclical chaotic intervals to 8-cyclical chaotic intervals for the map ψ. Indeed, as proved in [7], the point $(\alpha, \beta) = (1, -1)$ is an accumulation point for the curves related to the transition from 2^{i-1}-cyclical chaotic intervals to 2^i-cyclical chaotic intervals, $i = 2, \ldots$. The bifurcation curves related to the existence and stability of a cycle of period 3 can also be seen, and it is not intersected by the curve $\mathcal{B}$ (which is of interest to us). The "end point" for the curve $\mathcal{B}$ for our map is $(\alpha, \beta) = (1, 1 - e)$ corresponding to the parameter value $\sigma = \infty$ (or $\theta = e$).

It is clear that the curve $\mathcal{B}$ corresponds to the vertical line at $G = 1$ in the bifurcation diagram in the (G, σ)-parameter plane shown in Fig. 2, and the intersection points there evidenced: The point P corresponds to $\sigma = 2$ and the point α_i corresponds to σ_i, for $i = 4, 2, 1$.

To end our considerations we only have to get the approximate values of the coordinates of the intersection points α_i, $i = 4, 2, 1$, by using the analytical expressions of the bifurcation curves and, via (11), to get the corresponding values of the parameter σ. We obtain that $\sigma_4 \simeq 3.825$, $\sigma_2 \simeq 6.1226$ and $\sigma_1 \simeq 21.231$.

We have thus proved that, as G increases through 1, the border-collision bifurcation of the fixed point $x^* = 1$ can directly lead to a chaotic interval (for $\sigma > \sigma_1$), as in the example shown in Fig. 7b, or to 2-cyclical chaotic intervals (for $\sigma_2 < \sigma < \sigma_1$), as in the example shown in Fig. 7a, or to 4-cyclical chaotic intervals (for $\sigma_4 < \sigma < \sigma_2$), as in the example shown in Fig. 6b, or to a stable 2-cycle (for $2 < \sigma < \sigma_4$), as in the example shown in Fig. 6a. □

4. Economic interpretation and concluding remarks

To summarize the results proved in the previous section, we consider the example of dynamic behavior which can be obtained at $\sigma = 5$ representing the qualitative dynamics at any value of σ in the third interval of the theorem given in the previous section. In this case, we have $\theta = 2.441$ and for all G values in $(\theta - 1, \infty) = (1.441, \infty)$ the fixed point in the Romer regime is stable. As the values of G decreases, so that G enters the interval $(1, 1.441)$, the fixed point in the Romer regime is unstable, and one period-2 cycle also exists, stable for $G \in (1.0725, 1.441)$, while for $G \in (1, 1.0725)$ the 2-cycle is also unstable. Unlike the well-known period-doubling bifurcation scenario, the period-4 cycle that emerges cannot be stable, and instead the attractor of the system is a 4-cyclical chaotic interval, as illustrated in Fig. 6b. That is, for $G \in (1, 1.0725)$, in very few iterations any trajectory enters the four chaotic intervals, whose boundaries are completely known, as they are defined by the value of G and its first seven iterates. Thus, the width of such intervals depends on G. It is zero for $G = 1$ and $G = 1.0725$, while in between their width first increases and then decreases. We notice that if all the values of G for which the 2-cycle is stable (that is, $G \in (1.0725, 1.441)$) are considered to be plausible, then we are led to think that also some values in the interval $(1, 1.0725)$ must also be plausible, and therefore the chaotic regime is empirically plausible in this model. Once a point is inside the full-measure set of chaotic intervals, they are cyclically visited in the sequence $I_1 \to I_2 \to I_3 \to I_4 \to I_1$ as shown in Fig. 6b. We can notice that in this case the intervals are very thin, and specially close to the bifurcation values the trajectories look like 4-periodic, and thus in terms of predicting the set of values for x there is not much difference. Also when the width of the intervals is the widest, we can predict the interval inside which the orbit will be step by step, although inside it we can say nothing: It behaves as if subject to a random process, in this case due to a shock endogenously represented by the deterministic model.

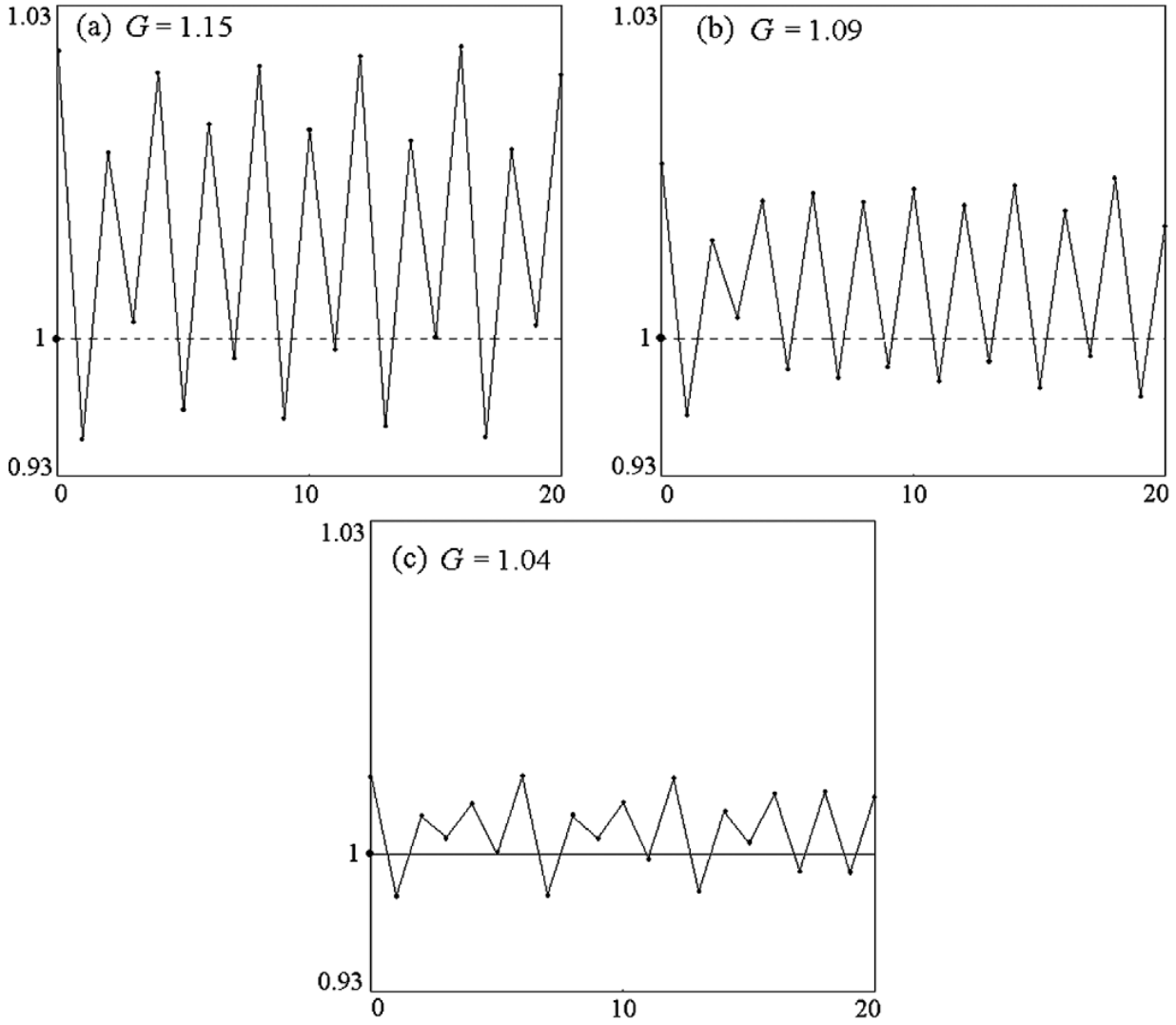

Fig. 10. Versus time trajectory at $\sigma = 15$ and $G = 1.15$ in (a); $G = 1.09$ in (b); $G = 1.04$ in (c).

The comments are similar, with obvious changes, for values of σ in the other interval, for example at $\sigma = 15$ (which represents the qualitative dynamics at any value of σ in the fourth interval of the theorem). In this case we can appreciate the difference between periodic and aperiodic dynamics, as we can see in Fig. 7a. As shown in that figure, the chaotic intervals are visited by a generic trajectory in the sequence $I_1 \to I_2 \to I_3 \to I_4 \to I_1$ when 4-periodic, and in the sequence $I_1 \to I_2 \to I_1$ when 2-periodic. In the last case the boundaries of the chaotic intervals are given by G and its first three iterates. We do not know whether high values of σ (such as $\sigma = 15$ or $\sigma = 20$) are indeed empirically plausible. If yes, this may lead to some uncertainty in the predictability of the model. In fact, when the trajectory belongs to a chaotic interval, we can predict which one will be visited, but nothing else. In this case we can say, for example, that a Solow regime is always followed by a Romer regime, while a trajectory may persist in a Romer regime at most for three periods, when the intervals are 4-cyclic. This can be seen in Fig. 10 where we keep $\sigma = 15$ and show the versus time values of x for 20 periods starting from the critical point G, at different G values; The dashed line at 1 denotes the separation between the Solow and Romer regime. In Fig. 10a the trajectory belongs to the 4-cyclic chaotic intervals.

The prediction is more difficult when the intervals are 2-cyclic, because in this case a trajectory may persist in a Romer regime (although changing intervals) also for three or more periods. How-

ever, the global absorbing interval is $[g(G), G]$ and it shrinks to the point 1 as G approaches 1. Thus the oscillations tend to be closer and closer to this value. This can be seen in Fig. 10 where we keep the same scale to appreciate the qualitative difference. In Fig. 10b, the trajectory belongs to the 2-cyclic chaotic intervals still quite far from the value of 1, while Fig. 10c shows a trajectory still in the 2-cyclical chaotic intervals but at $G = 1.04$. We can see that in any case the states assume values very close to 1.

Acknowledgments

The authors thank the anonymous referees for the useful suggestions and comments, which allowed us to improve the presentation of the results.

References

[1] S. Banerjee, M.S. Karthik, G. Yuan, J.A. Yorke, Bifurcations in one-dimensional piecewise smooth maps—Theory and applications in switching circuits, IEEE Trans. Circuits Syst.-I: Fund. Theory Appl. 47 (3) (2000) 389–394.
[2] R. Devaney, An Introduction to Chaotic Dynamical Systems, The Benjamin/Cummings Publishing Co., Menlo Park, California, 1986.
[3] M. di Bernardo, M.I. Feigen, S.J. Hogan, M.E. Homer, Local analysis of C-bifurcations in n-dimensional piecewise smooth dynamical systems, Chaos Solitons Fractals 10 (11) (1999) 1881–1908.
[4] L. Gardini, Homoclinic bifurcations in n-dimensional endomorphisms, due to expanding periodic points, Nonlinear Anal. 23 (8) (1994) 1039–1089.
[5] C. Halse, M. Homer, M. di Bernardo, C-bifurcations and period-adding in one-dimensional piecewise-smooth maps, Chaos Solitons Fractals 18 (2003) 953–976.
[6] C.H. Hommes, H. Nusse, Period three to period two bifurcations for piecewise linear models, J. Econ. 54 (2) (1991) 157–169.
[7] Y.L. Maistrenko, V.L. Maistrenko, L.O. Chua, Cycles of chaotic intervals in a time-delayed Chua's circuit, Internat. J. Bifur. Chaos 3 (6) (1993) 1557–1572.
[8] Y.L. Maistrenko, V.L. Maistrenko, S.I. Vikul, On period-adding sequences of attracting cycles in piecewise linear maps, Chaos Solitons Fractals 9 (1) (1998) 67–75.
[9] K. Matsuyama, Growing through cycles, Econometrica 67 (2) (1999) 335–347.
[10] T. Mitra, A sufficient condition for topological chaos with an application to a model of endogenous growth, J. Econ. Theory 96 (2001) 133–152.
[11] A. Mukherji, Robust cyclical growth, Internat. J. Econ. Theory 1 (2005) 233–246.
[12] H.E. Nusse, J.A. Yorke, Border-collision bifurcations including period two to period three for piecewise smooth systems, Phys. D 57 (1992) 39–57.
[13] H.E. Nusse, J.A. Yorke, Border-collision bifurcations for piecewise smooth one-dimensional maps, Internat. J. Bifur. Chaos 5 (1) (1995) 189–207.
[14] I. Sushko, A. Agliari, L. Gardini, Bistability and border-collision bifurcations for a family of unimodal piecewise smooth maps, Discrete Contin. Dyn. Syst. Ser. B 5 (3) (2005) 881–897.
[15] I. Sushko, A. Agliari, L. Gardini, Bifurcation structure of parameter plane for a family of unimodal piecewise smooth maps: Border-collision bifurcation curves, Chaos Solitons Fractals 29 (3) (2006) 756–770.